The Effect of Spike Redistribution in a Reciprocally Connected Pair of Neurons with Spike Timing-Dependent Plasticity

Gerardina Hernández*

Intelligent Systems Program, University of Pittsburgh, Pittsburgh, PA 15260

Jonathan Rubin†

Department of Mathematics, University of Pittsburgh, Pittsburgh, PA 15260

Paul Munro‡

School of Information Science, University of Pittsburgh, Pittsburgh, PA 15260

October 18, 2002

Abstract. This work considers a system of two spike-response cells, mutually connected by excitatory synapses that modify according to a multiplicative form of spike timing-dependent plasticity (STDP). The units are driven by independent external inputs and one common input, representing a global cortical rhythm. Our simulations show that the synaptic weights converge to attractors that encode input and plasticity parameters, independent of initial conditions. In certain parameter regimes, the temporal correlation induced by coupling and the shared cortical signal lead to redistribution of spikes to favor doublets. When this occurs, the weight changes associated with these doublets dominate convergence of weights to their attractors. Thus, spike timing-dependent plasticity can allow subsets of spikes to play a predominant role in the evolution of synaptic weights.

Keywords. Spike timing-dependent plasticity, synaptic weights, spike redistribution

*Current address: Highmark Blue Cross Blue Shield, Fifth Avenue Place, 120 Fifth Avenue, Ste. P7205, Pittsburgh, PA 15222-3099; gerardina.hernandez@highmark.com

†Partially supported by NSF grants DMS-9804447 and DMS-0108857; member of the Center for the Neural Basis of Cognition; rubin@math.pitt.edu

‡pmunro@mail.sis.pitt.edu

1 Introduction and Model

Spike timing-dependent plasticity (STDP) is characterized by synaptic weight changes that depend on the precise timing of spikes fired by pre- and post-synaptic cells. Past computational studies have tallied changes in synaptic weights due to STDP by treating all timing differences within the timing window as relevant. Recently, the suggestion has been made that data on STDP may be better represented by a rule in which only certain pre- and post-synaptic spike pairs are counted [8, 2].

We simulate two neurons, a and b, mutually connected by positive weights W_{ab} and W_{ba} (the first subscript denotes the presynaptic cell). Each neuron is governed by the spike response model [3], which is an instance of a "threshold-fire model." A spike train is characterized by the set of firing times $Z_x = \{t_x^1, ..., t_x^n\}$, with $t_x^i < t_x^j$ for $i < j$, where t_x^i is the ith firing time of neuron x. A neuron generates a spike when its membrane potential crosses a threshold θ. Here, membrane potential refers to the internal state $u_i(t)$ of a neuron i at time t, defined by

$$u_i(t) = \sum_{t_i^z \in Z_i} \eta_i(t - t_i^z) + \sum_j \sum_{t_j^z \in Z_j} W_{ji}\pi_{ji}(t - t_j^z) + w_i h_i(t) + w_{ctx} h_{ctx}(t) \qquad (1)$$

for $t > \max\{\max(Z_i), \max(Z_j)\}$. In equation (1), a presynaptic spike at time t_j^z contributes an amount $W_{ji}\pi_{ji}(t - t_j^z)$ to the state u_i at time t. The weight W_{ji} is the strength of the corresponding connection, dynamically derived from a multiplicative spike timing-dependent learning process described below. The positively-valued kernel π_{ji} describes the time course of an excitatory postsynaptic potential. The negatively-valued kernel η_i in (1) describes the neuron's response to its own firing (reset of the membrane potential after each spike, together with neuronal refractoriness); see [3] for details. The term $h_i(t)$ represents a Poisson input signal, with fixed weight w_i; we will use f_i to denote the frequency of this signal. Finally, $h_{ctx}(t)$ is a periodic context signal, with weight w_{ctx}, applied to both cells in the network. This shared context signal represents a global cortical rhythm; such rhythms are associated with cognitive tasks (13 Hz sensory-motor rhythm: see [7, 4]; 40 Hz gamma rhythm: reviewed in [1]).

Let τ denote the time at which a presynaptic spike occurs minus the time of a postsynaptic spike. To represent the temporally-dependent potentiation (LTP) and depression (LTD) kernels for STDP, we define $K_s(\tau) = \beta_s|\tau|e^{-\alpha_s|\tau|}$ where $s = P$ for $\tau < 0$, $s = D$ for

$\tau \geq 0$, and where $\alpha_P, \alpha_D, \beta_P > 0$ and $\beta_D < 0$. In our simulations, the transition between maximal potentiation and depression is 10 msec. The kernel parameters are $\alpha_P = 0.5$, $\alpha_D = 0.125$, $\beta_P = \alpha_P$ and $\beta_D = -0.18\alpha_D$.

We implement a multiplicative spike timing-dependent learning rule (mSTDP) which implicitly constrains weights between bounds $0 \leq \Omega_{min} < \Omega_{max}$. When the most recent presynaptic spike t_j^n occurs before the most recent postsynaptic spike t_i^m, the weight from cell j to cell i is potentiated according to

$$\Delta W_{ji}(t_i^m) = \lambda[\Omega_{max} - W_{ji}(\max\{t_i^{m-1}, t_j^n\})][\sum_{z=1}^{n}(K_P(t_j^z - t_i^m))], \tag{2}$$

where λ denotes a learning rate. When the most recent postsynaptic spike t_i^m fires before the most recent presynaptic spike t_j^n, the weight from j to i is depressed according to

$$\Delta W_{ji}(t_j^n) = \lambda[W_{ji}(\max\{t_i^m, t_j^{n-1}\}) - \Omega_{min}][\sum_{z=1}^{m}(K_D(t_j^n - t_i^z))]. \tag{3}$$

If $t_i^m = t_j^n$ computationally, then both equations (2) and (3) are implemented, with $\max\{t_i^{m-1}, t_j^{n-1}\}$ used as the argument of W_{ji} on the right hand side of both. In our simulations, we take $\lambda = 0.1$, $\Omega_{max} = 2$, $\Omega_{min} = 0$, unless otherwise noted.

2 Results

2.1 Existence and properties of attractors

For fixed parameter values, the weights W_{ab}, W_{ba} of the excitatory synapses between the neurons converge under mSTDP to a fixed attractor in the (W_{ab}, W_{ba}) plane, irrespective of the initial weight values used. An example appears in Figure 1, which shows trajectories of weights, both in the (W_{ab}, W_{ba}) plane and as functions of time.

The weight values in the attractor do depend on the intrinsic parameters and driving signals in the network. In particular, the input and context frequencies, the input and context weights, and the relative areas of the LTP and LTD kernels are encoded by the attractor mean, while the specific spike times in a particular spike train influence the details of the convergence to the attractor. These results hold with or without a context signal. An example illustrating the role of driving frequencies is shown in the upper left of Figure 2. Additional examples appear in [6, 5].

2.2 Redistribution of spikes

The properties of the weight attractors, as well as the mechanisms underlying these results, will be further detailed elsewhere [6, 5]. For our purposes here, it is important to note that the temporal correlation mechanisms of coupling and a shared context signal lead to redistribution of spikes, relative to baseline firing of uncoupled cells due to their independent Poisson inputs. The degree of redistribution depends on the parameter regime simulated. For example, when w_{ctx} is weak, we find little redistribution. When the context signal frequency is 13 Hz and w_{ctx} is large, the nature of the spike redistribution depends on the frequencies of the independent driving signals $h_a(t), h_b(t)$. The interspike interval (ISI) plots on the bottom row of Figure 2 show that high input frequencies f_a, f_b to both cells cause a shift of ISI's toward lower values, corresponding to a tendency for both cells in the network to fire spike doublets; this is not observed with low frequency drives to the cells or with context frequency of 40 Hz. When w_{ctx} is large, cells are entrained to fire together in response to most context signals, and the relatively low context frequency in the 13 Hz case allows them to recover sufficiently between signals to fire independent spikes, which may become doublets when context signals follow soon afterward. Further, the coupling between cells leads to a high probability that a doublet of one cell will elicit a doublet from the other, as illustrated in the spike trains in the upper right of Figure 2.

2.3 Computations with a spike subset

To explore the role of doublets in the simulated recurrent network, we computed weight changes using a computational rule that only includes doublets. To do this, we examined the spike train of cell a, computed the ISI's between each pair of consecutive spikes, and kept only the spike pairs from the bottom 25% of the cell's ISI distribution. For each such pair, call them t_a^1, t_a^2, we formed a subset of postsynaptic spikes consisting of the last postsynaptic spike before t_a^1, the first postsynaptic spike after t_a^2, and all postsynaptic spikes between these. We then computed the changes in W_{ab} prescribed by our learning kernel for the interactions of each of t_a^1, t_a^2 with each spike in the postsynaptic subset; see Figure 3. This gave an evolution of W_{ab} based on fewer than 25% of the spikes fired by the network. A symmetric procedure was used to compute the evolution of W_{ba}.

To evaluate how well the doublet procedure reproduces the weight changes seen with the full spike set, we also performed a control experiment. In the control, the same number of

presynaptic spikes was used as in the doublet procedure, but these were selected randomly. The postsynaptic subset for a presynaptic spike consisted of the two postsynaptic spikes closest in time to the presynaptic one. The relative error between the original weights W_{ij} and the weights W_{ij}^p generated by procedure p was computed for both the doublet and the control procedures as $E_{ij}^p = \frac{1}{n}\sum_{z=1}^{n} |W_{ij}(z) - W_{ij}^p(z)|/W_{ij}(z)$ for z ranging over all spike times (of both cells) in the full spike set.

We found that the doublet procedure always led to convergence of weights to the original attractor region (Figure 4). Further, a key point, also illustrated in Figure 4, is that the weight values in the doublet procedure tracked the original weight values much better than expected by chance: the relative errors in both weights with the doublet procedure were approximately 2%, and these errors were found to be significantly smaller than those for the control procedure over 20 simulations with fixed parameters, as measured by a one-tailed t-test ($p < 0.0005$). The reliable reconstruction of original weight values by the doublet procedure implies that for learning events which occur over a short time period, when weights may be far from attractor values, evolution of weights is still dominated by effects of spike doublets.

3 Conclusions

The existence of weight attractors provides a synaptic encoding of incoming stimuli that combines rate information, encoded in attractor values, with temporal information, encoded in particular spike times. Our principal finding is that, in parameter regimes in which spikes are redistributed, by coupling and common context signals, to favor spike doublets, the dynamics of the weights as they converge to these attractors is dominated by the effects of these doublets. This arises simply from applying the learning rule (2), (3). Thus, in addition to driving downstream units, bursts may induce longer-term effects on network behaviors.

Recent results indicate that the combined effect of multiple spikes is more complex than had previously been assumed [8, 2], and experimental data may be better modeled by computational versions of STDP that do not count all spikes than by applications of STDP rules to complete spike sets [8]. Clearly, the explanation of this finding must involve the fact that different spiking patterns induce different responses in cellular machinery (calcium channels, NMDA receptors, and so on). Nonetheless, our results show that even

a fixed STDP rule, which does not take into account the involvement of such factors, can allow a certain subset of spikes to play a predominant role in driving weight dynamics when sufficient spike redistribution occurs.

References

[1] A. Engel, P. Fries & W. Singer, Dynamic predictions: oscillations and synchrony in top-down processing, Nat. Neurosci. Rev. 2 (2001) 704–716.

[2] R.C. Froemke & Y. Dan, Spike timing dependent synaptic modification induced by natural spike trains, Nature, 416 (2002) 433–438.

[3] W. Gerstner, Spiking neurons, in W. Maass & C. M. Bisshop, ed., Pulsed Neural Networks (MIT Press, Cambridge, MA, 1999).

[4] D. Giannitrapani, The electrophysiology of intellectual functions (Karger, Basel, 1985).

[5] G. Hernández, Spike-timing-dependent plasticity under temporal correlation mechanisms, Ph.D. Thesis, Intelligent Systems Program, University of Pittsburgh, 2001.

[6] G. Hernández, P. Munro & J. Rubin, in preparation.

[7] J.O. Lubar & J.F. Lubar, Electroencephalographic biofeedback of SMR and beta for treatment of attention deficit disorder in a clinical setting, Biofeedback and Self-Regulation, 9 (1984) 1–23.

[8] P. Sjöström, S. Nelson & G. Turrigiano, Rate, timing, and cooperativity jointly determine cortical synaptic plasticity, Neuron, 32, (2002) 1149–1164.

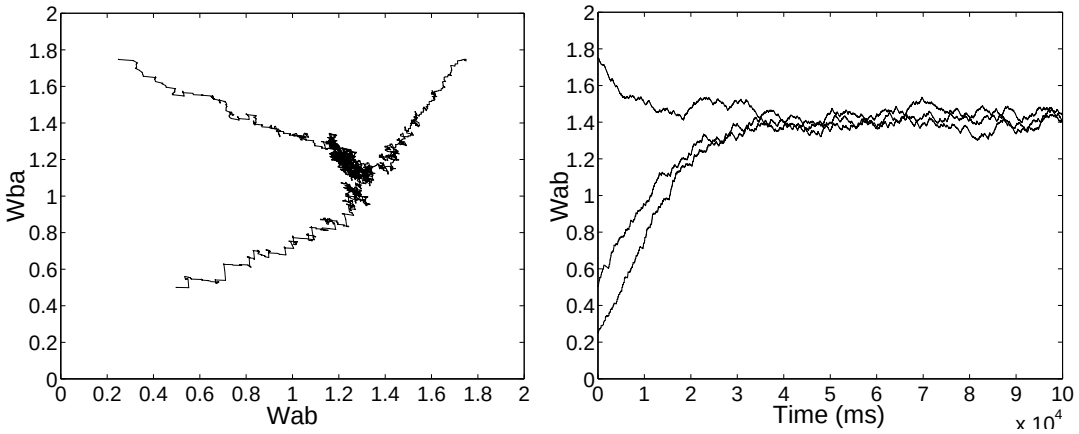

Figure 1: *Attractors for weights are independent of initial conditions. Left: Evolution of both weights from three different initial conditions, with input frequencies* $f_a = 11$ *Hz,* $f_b = 37$ *Hz and 13 Hz context frequency. Right: Time evolution of* W_{ab} *for different initial values.*

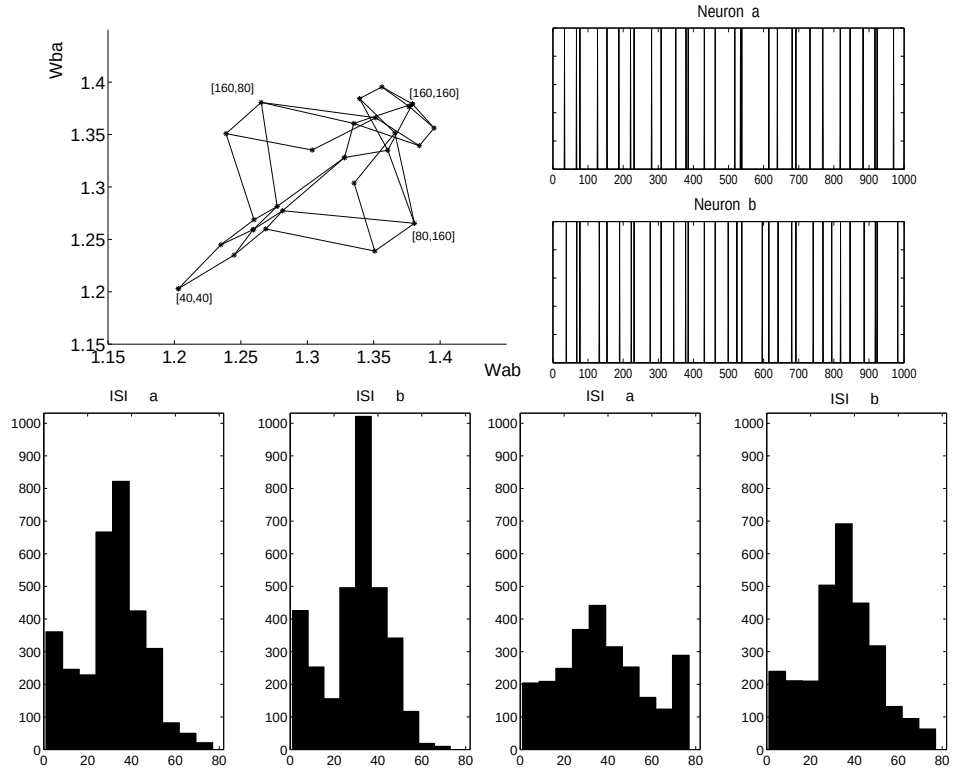

Figure 2: *Spike redistribution with 13 Hz context signal and strong w_{ctx} ($w_{ctx} = 15$). Top left: Mean attractor values. Different points correspond to different drive frequencies (f_a, f_b). Top right: Segments from spike trains (vertical lines denote spikes) of both cells in the large f_a, f_b regime, which favors doublets, often at similar times in both cells. Bottom row: Distributions of interspike intervals for neuron a (ISI_a) and neuron b (ISI_b). Left plots show a redistribution toward small ISI's for large f_a, f_b. Right plots show that this redistribution does not occur for small f_a, f_b.*

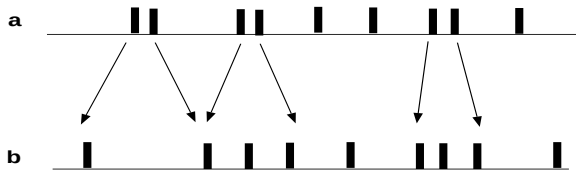

Figure 3: *Schematic representation of the selection of a subset of spikes. A subset of spikes from cell a are selected, corresponding to small ISI's, and then weight changes are computed from their interactions only with the spikes of cell b that are closest in time (between the arrows for each pair).*

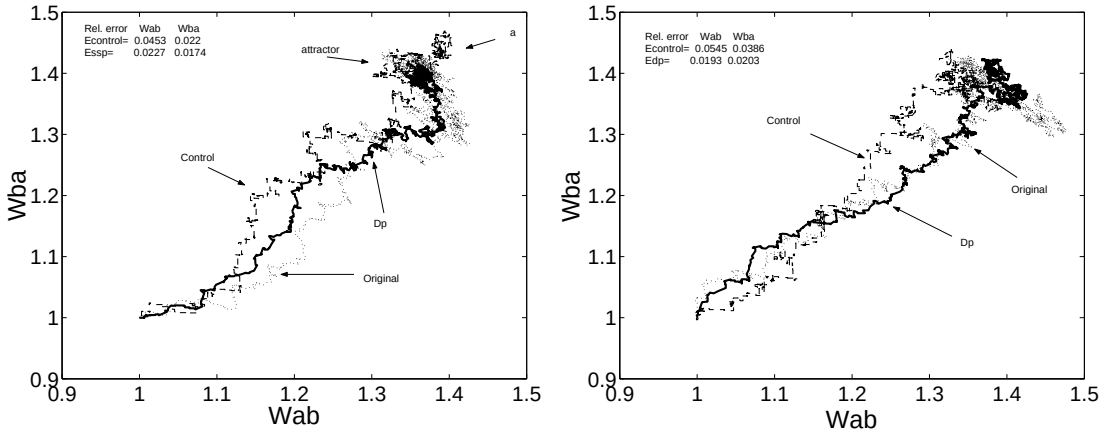

Figure 4: *Tracking of weight changes from a full simulation (Original - dotted curve) by the doublet procedure (Dp - solid curve) and the control procedure (Control - dashed curve). The input frequencies were 160Hz to neuron a and 200Hz to neuron b, with learning rate* $\lambda = 0.02$. *Top: The control procedure converges to region "a" rather than to the attractor region below it. Top and bottom: The doublet procedure tracks the weight changes from the full simulation better than the control procedure does; corresponding errors* $(E_{control}, E_{dp})$ *are displayed in the upper left of each plot.*